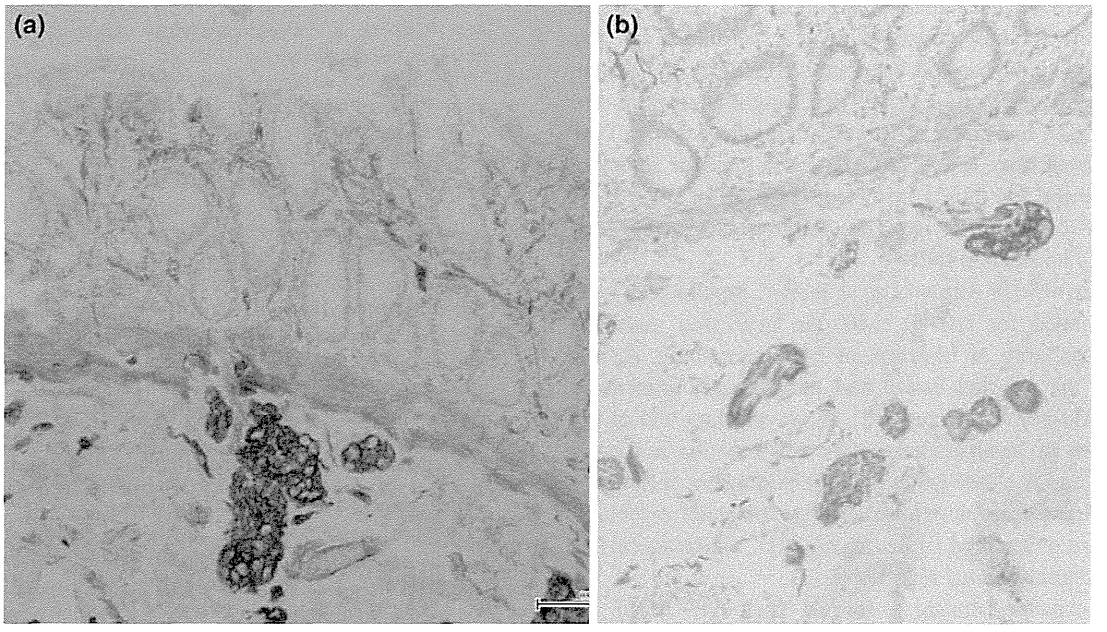

Fig. 4 The histological findings of Case 4. **a** AChE staining at 6 months of age showed giant ganglia present in the submucosa and AChE-positive nerve fibers in the lamina propria. **b** AchE staining at 2y 9m showed the persistence of giant ganglia and hyperganglionosis in the submucosa. AchE-positive fibers were not prominent in the lamina propria. The density and number of ganglion cells were lower compared with those at 6 months

IND cases have mainly been reported in Europe, and the incidence in Europe has been noted to be very high in some reports [15]. In contrast, IND cases have rarely been reported in the USA. Some pediatric surgeons in the USA have pointed out that strict descriptions of IND were lacking in the European reports, and the disease should not yet be accepted as a definite clinical entity [16]. The 4th International Symposium on Hirschsprung's Disease and Related Neurocristopathies in 2004, which many leading pediatric surgeons from the USA and European countries attended, reached the consensus that: (1) almost all of the participants believe that IND does exist. (2) Some believe in the presently defined diagnostic criteria, whereas others suggest that these diagnostic criteria are not sufficiently reliable. (3) Some participants question whether IND is a truly separate entity or is an acquired secondary phenomenon related to long-standing constipation or chronic obstruction [17].

Further pathological examinations have shown that giant ganglia are present in the submucosa of the normal neonate and infant, and gradually decrease during development. The AchE activity in the lamina propria mucosae has been shown to be age dependent, and disappears upon the maturation of the submucosal plexus [18]. Ectopic ganglion cells in the lamina propria and AchE-positive fibers around the vessels are also sometimes seen in the normal mucosa of the intestine (personal experience). The criteria for giant ganglia have been changed. The number of nerve cells per ganglion had already been noted to be three to five in controls [19], therefore, the initial criterion for giant ganglia proposed by Kobayashi was five or more ganglion cells [20]. The number was then increased to more than seven [21], and then finally nine or more [1, 11, 12]. The criteria for IND-B have been gradually revised by the Meier-Ruge group to the current diagnostic criteria [(1) more than 20 % of 25 submucosal ganglia contain nine or more ganglion cells and (2) the patient must be older than 1 year]. They recommend that the diagnosis of IND-B should be avoided in the first year of life due to the potential of a misdiagnosis in infants [1, 11, 12].

In our study, there were only four "true" cases of IND-B matching the most current criteria treated during a 10-year period in Japan. All of them showed giant ganglia in the submucosa, and three out of the four cases underwent surgical resection of the left colon. The histology of full-thickness resected specimens showed apparent hyperplasia of myenteric plexus, mimicking ganglioneuromatosis. Some of the submucosal plexus showed similar findings. Based on these findings, giant ganglia in the submucosa may indicate the presence of ganglioneuromatosis-like hyperplasia of the myenteric plexus, which may cause motility disorders. Similar cases had already been reported in a child in Austria in 1981 [22], as well as in an adult in the USA in 1984 [23]. In 2003, there was one case of neurofibromatosis

type I (NF-1) associated with IND-B who was bothered by chronic episodic constipation and diarrhea [24]. This patient was a 4-year and 8-month-old male from Taiwan. Friedmacher and Puri described that ganglioneuroma is one of the VHD, and most of these patients have MEN Type II-associated disease [25, 26]. None of the four Japanese cases showed any family history or evidence of MEN Type II- or NF-1-related disease. Therefore, our cases were considered to be isolated IND-B.

Conservative treatment for at least 6 months has been recommended for IND-B, with the next step generally being myectomy or injection of botulinum toxin. Resections of the affected bowel and pull-through procedures have rarely been indicated [12]. However, three out of the four cases in Japan underwent bowel resection and pull-through, and one case underwent the permanent colostomy. Our Japanese cases with apparent hyperplasia of myenteric plexus are considered to be "true" IND, which more frequently requires bowel resection.

In conclusion, during a 10-year period in Japan, 13 cases matched the classical criteria for IND-B, and 45 % (7/13) of these cases underwent surgical procedures. However, only four cases could be diagnosed with IND-B based on the current criteria, and 75 % (3/4) of these required intestinal resection and pull-through. Most of the cases also required further conservative treatment. IND-B cases matching the current criteria are considered to be quite rare, and are associated with marked hyperplasia of myenteric plexus mimicking ganglioneuromatosis. Most of them required surgical treatment and further medical treatment. Therefore, "true" IND-B is suggested to be a rare and intractable disease.

Acknowledgments This study was supported by a grant from The Ministry of Health, Labor Sciences Research Grants for Research on intractable disease. The authors thank The Japanese Society of Pediatric Surgeons, The Japanese Society of Pediatric Nutrition, Gastroenterology and Nutrition and The Japanese Study Group of Pediatric Constipation. The authors thank Dr. Bryan Quinn for reading the manuscript, and also thank Ms. Masutomi and the Yamazaki Department of Pediatric Surgery, Kyushu University, for their help in processing the data.

References

1. Hirschsprung's Disease and Allied Disorders (2008) 3rd ed. Holschneider A and Puri P (ed). Springer
2. Ravitch MM (1958) Pseudo Hirschsprung's disease. Ann Surg 147:781–795
3. Bentley JFR, Nixon HH, Ehrenpreis TH, Spencer B (1966) Seminar on pseudo-Hirschsprung's disease and related disorders. Arch Dis Child 41:143–154
4. Puri P (1997) Variant Hirschsprung's disease. J Pediatr Surg 32:149–157
5. Okamoto E and Toyosaka A (1996) Pseudo-Hirschsprung's disease. Research on the pathophysiology, diagnosis and treatment (in Japanese) Nagai-Shoten
6. Maldonaldo JE, Greegg JA, Green PA, Brown AL (1970) Chronic idiopathic intestinal pseudo-obstruction. Am J Med 49:203–212
7. Meier-Ruge W (1971) Casuistic of colon disorder with symptoms of Hirschsprung's disease. Verh Dtsch Ges Pathol 55:506–510
8. Fadda B, Maier WA, Meier-Ruge W et al (1983) Neuronal intestinal dysplasia. Critical 10-years' analysis of clinical and biopsy diagnosis. Z Kinderchir 38:305–311
9. Puri P, Rolle U (2004) Variant Hirschsprung's disease. Semin Pediatr Surg 13:293–299
10. Puri P, Lake BD, Nixon HH et al (1977) Neuronal colonic dysplasia: an unusual association of Hirschsprung's disease. J Pediatr Surg 12:681–685
11. Meier-Ruge WA, Ammann K, Bruder E et al (2004) Updated results on intestinal neuronal dysplasia (IND B). Eur J Pediatr Surg 14:384–391
12. Friedmacher F, Puri P (2013) Classification and diagnostic criteria of variants of Hirschsprung's disease. Pediatr Surg Int 29:855–872
13. Kanamori Y, Hasizume K, Sugiyama M et al (2005) Type B intestinal neuronal dysplasia. Pediatr Int 47:338–340
14. Goldblum JR, Folpe AL, Weiss SW. Benign tumors of peripheral nerves. In: Enzinger and Weiss's Soft Tissue Tumors, 6th ed. Philadelphia, PA, Elsevier Saunders; 2014:786–789
15. Lake BD (1995) Intestinal neuronal dysplasia. Why does it only occur in parts of Europe? Virchows Arch 426:537–539
16. Csury L, Pena A (1995) Intestinal neuronal dysplasia. Myth or reality? Literature review. Pediatr Surg Int 10:441–446
17. Martucciello G, Pini Prato A, Puri P, Holschneider AM, Meier-Ruge W et al (2005) Controversies concerning diagnostic guidelines for anomalies of the enteric nervous system: a report from the fourth International Symposium on Hirschsprung's disease and related neurocristopathies. J Pediatr Surg 40:1527–1531
18. Coerdt W, Mivhel JS, Rippin G et al (2004) Quantitative morphometric analysis of the submucous plexus in aged-related control groups. Virchows Arch 444:239–246
19. Meier-Ruge WA, Bronnimann PB, Gambazzi F et al (1995) Histopathological criteria for intestinal neuronal dysplasia of the submucosal plexus (type B). Virchows Arch 426:549–556
20. Kobayashi H, Hirakawa H, Puri P (1995) What are the diagnostic criteria for intestinal neuronal dysplasia. Pediatr Surg Int 10:459–464
21. Meier-Ruge W, Gambazzi F, Kaufeler RE et al (1994) The neuropathological diagnosis of neuronal intestinal dysplasia (NID B). Eur J Pediatr Surg 4:267–273
22. MacMahon RA, Moore CCM, Cussen LJ (1981) Hirschsprung-like syndromes in patients with normal ganglion cells on suction rectal biopsy. J Pediatr Surg 16:835–839
23. Feinstat T, Tesluk H, Schuffler MD et al (1984) Megacolon and neurofibromatosis: a neuronal intestinal dysplasia. Gastroenterology 86:1573–1579
24. Wu JF, Chen HL, Peng SS et al (2003) Neurofibromatosis type 1 and intestinal dysplasia type B in a child: report of one case. Acta Paediatr Taiwan 44:232–234
25. Cohen MS, Phay JE, Albinson C et al (2002) Gastrointestinal manifestations of multiple endocrine neoplasia type 2. Ann Surg 235:648–654
26. King SK, Southwell BR, Hutson JM (2006) An association of multiple endocrine neoplasia 2B, a RET mutation; constipation; and low substance P –nerve fiber density in colonic circular muscle. J Pediatr Surg 41:437–442

Pediatr Surg Int (2014) 30:907–914
DOI 10.1007/s00383-014-3576-9

ORIGINAL ARTICLE

Therapeutic potential of mesenchymal stem cell transplantation in a nitrofen-induced congenital diaphragmatic hernia rat model

Ratih Yuniartha · Fatima Safira Alatas · Kouji Nagata · Masaaki Kuda · Yusuke Yanagi · Genshiro Esumi · Takayoshi Yamaza · Yoshiaki Kinoshita · Tomoaki Taguchi

Accepted: 15 July 2014 / Published online: 5 August 2014

Abstract
Purpose The aim of this study was to evaluate the efficacy of mesenchymal stem cells (MSCs) in a nitrofen-induced congenital diaphragmatic hernia (CDH) rat model.
Methods Pregnant rats were exposed to nitrofen on embryonic day 9.5 (E9.5). MSCs were isolated from the enhanced green fluorescent protein (eGFP) transgenic rat lungs. The MSCs were transplanted into the nitrofen-induced E12.5 rats via the uterine vein, and the E21 lung explants were harvested. The study animals were divided into three: the control group, the nitrofen-induced left CDH (CDH group), and the MSC-treated nitrofen-induced left CDH (MSC-treated CDH group). The specimens were morphologically analyzed using HE and immunohistochemical staining with proliferating cell nuclear antigen (PCNA), surfactant protein-C (SP-C), and a-smooth muscle actin.
Results The alveolar and medial walls of the pulmonary arteries were significantly thinner in the MSC-treated CDH group than in the CDH group. The alveolar air space areas were larger, while PCNA and the SP-C positive cells were significantly higher in the MSC-treated CDH group, than in the CDH group. MSC engraftment was identified on immunohistochemical staining of the GFP in the MSC-treated CDH group.
Conclusions MSC transplantation potentially promotes alveolar and pulmonary artery development, thereby reducing the severity of pulmonary hypoplasia.

Keywords Mesenchymal stem cells · Congenital diaphragmatic hernia · Pulmonary hypoplasia · Pulmonary hypertension

R. Yuniartha · F. S. Alatas · K. Nagata (&) · M. Kuda · Y. Yanagi · G. Esumi · Y. Kinoshita · T. Taguchi
Department of Pediatric Surgery, Reproductive and Developmental Medicine, Graduate School of Medical Sciences, Kyushu University, Fukuoka, Japan
e-mail: koujin@pedsurg.med.kyushu-u.ac.jp

F. S. Alatas
Department of Child Health, Faculty of Medicine, Cipto Mangunkusumo Hospital, Universitas Indonesia, Jakarta, Indonesia

T. Yamaza
Department of Molecular Cell and Oral Anatomy, Faculty of Dental Science, Kyushu University, Fukuoka, Japan

Introduction

According to recent advances in postnatal therapy, there have been several reports of improvements in the treatment outcomes of congenital diaphragmatic hernia (CDH) [1, 2]. However, CDH patients with severe pulmonary hypoplasia continue to exhibit high morbidity and mortality. Pulmonary hypoplasia, defined as arrest in lung development, is characterized by decreased airway branching, thickened alveolar walls, increased interstitial tissue and decreased alveolar air space [3, 4]. In experimental animal models of CDH, several treatments, such as the prenatal administration of growth factor, vitamin E and retinoid acid, have suggested to improve lung hypoplasia [4–6]. However, despite the introduction of new drugs and changes in management, limitations persist, and these therapies appear to be far from being able to truly cure lung hypoplasia.

Currently, the efficacy of a type of prenatal intervention, named percutaneous fetoscopic endoluminal tracheal occlusion (FETO) therapy, is being investigated in the tracheal occlusion to accelerate lung growth trial [(TOTAL); a European and North American collaboration]

[7]. The use of FETO remains controversial, as some papers have reported improvements in the survival of patients with severe CDH, although neonates and infants treated with this therapy subsequently display obvious tracheomegaly [7–9]. Therefore, it may be necessary to combine additional experimental therapies, such as cellular therapy and tissue engineering approaches, to reduce the risk of harmful complications [7, 10].

Mesenchymal stem cells (MSCs) are widely used in experimental research as a source of cell-based therapy. MSCs are known to be self-renewing, with the ability to form an adherent cell layer in a plastic standard culture dish and exhibit a combination of phenotypic and functional characteristics [11]. MSCs can be isolated from the stromal tissues of various adult organs, including bone marrow, muscle, amniotic fluid, adipose tissue and the dermis and lungs [11, 12]. MSCs also display specific characteristics, which are able to self-renew and differentiate into osteocytes, chondrocytes, adipocytes, myofibroblasts, and smooth muscle cells (multipotent differentiation) [12]. Other characteristics of MSCs include their fibroblast-like shape in culture, extensive capacity for proliferation and negative for hematopoietic stem cells (HSCs) and endothelial cell surface marker [10–13]. Their tendency to exhibit low immunogenicity may also make them appropriate for use in allogeneic transplantation [10, 13].

A number of studies have demonstrated the efficacy of MSC transplantation in treating pulmonary diseases, such as that observed in bleomycin, endotoxin, and lipopolysaccharide (LPS)-induced lung injury models [10, 14]. Aslam et al. [14] proposed that the application of bone marrow MSCs and their secreted factors offers the potential for new therapeutic approaches in cases of neonatal chronic lung disease.In addition, cellular therapies have been suggested to have favorable effects in improving serious pediatric lung diseases such as pulmonary hypoplasia and cystic fibrosis [7, 10, 15]. However, the efficacy and mechanisms of MSC transplantation in CDH models have not been fully clarified.

The aim of this study was, therefore, to evaluate the efficacy of MSC therapy in a nitrofen-induced CDH rat model, based on the detection of lung maturation and a reduction in the degree of pulmonary hypertension.

Materials and methods

Experimental animals

The animal experiments were approved by the Institutional Animal Care and Use Committee of Kyushu University (approval no. A-25-175-0). Pregnant Wistar rats were purchased from a commercial breeder (Japan Kyudo, Inc., Saga, Japan) and randomly divided into three groups: the control group (n = 6), the nitrofen-induced left CDH group (CDH group, n = 5), and the MSC-treated nitrofen-induced left CDH group (MSC-treated CDH group, n = 6). Pregnant rats in both the CDH and MSC-treated CDH groups were exposed intragastrically to 100 mg of nitrofen (2,4-dichlorophenyl-p-nitrophenyl ether, Wako, Japan), dissolved in olive oil on embryonic day 9.5 of gestation (E9.5), whereas those in the control group received vehicle only [4].

Isolation and culture of MSCs

Mesenchymal stem cells were isolated from the lungs of donor adult enhanced green fluorescent protein (eGFP) transgenic SD rats [SD-Tg(CAG-EGFP), Japan SLC Inc., Shizuoka, Japan]. The harvested lung tissues were flushed with phosphate-buffered saline (PBS) to wash out the blood, and the attached trachea and connective tissue were subsequently removed. The tissues were then minced, and treated with PBS containing 0.4 % collagenase type I (Worthington Biochemicals, Lakewood, NJ, USA) and 0.3 % dispase II (Sanko Junyaku, Tokyo, Japan) for 1 h at 37 °C. The digested samples were filtered using a 70-l m cell strainer (BD Bioscience, San Jones, CA, USA) to obtain a single-cell suspension. The cells were seeded at 1 9 10^6 cells in a 75-cm^2 tissue culture flask and incubated at 37 °C with 5 % CO_2. Twenty-four hours after incubation, non-adherent cells were removed by washing twice with PBS, and the adherent cells were cultured with a growth medium. The growth medium consisted of 20 % fetal bovine serum (FBS) (Equitech-Bio, Kerrville, TX, USA), 100 l M of L-ascorbic acid 2-phosphate (Wako Pure Chemical, Osaka, Japan), 2 mM L-glutamine (Nacalai Tesque, Kyoto, Japan), an antibiotic mixture containing 100 U/ml of penicillin and 100 l g/ml of streptomycin (Nacalai Tesque), and 250 ng/ml amphotericin B (Fungizone, Life technologies, USA) in alpha minimum essential medium (aMEM, Invitrogen, Grand Island, NY, USA). After reaching confluence, the adherent cells were harvested using 0.25 % trypsin and 0.1 mM EDTA solution, and reseeded at a density of 0.2 9 10^6 cells in 100-mm tissue culture dishes. The passaging of the cultured cells was repeated an additional two or four times to generate a sufficient number of cells for transplantation.

MSC transplantation

On E12.5, MSCs isolated from the lung tissues of the eGFP rats were transplanted into the fetuses. Under deep pentobarbital anesthesia (50 mg/kg, i.p.), MSCs suspended in PBS were intravenously injected via the uterine vein in the bilateral horn of the uterus of the dams, with a total of

15–20 9 10^6 MSCs injected. After the surgery, the graved rats were treated with 0.05 mg/kg buprenorphine (Torpan, Maillefer, Switzerland) as an analgesic, and kept in a temperature-controlled room with a 12-h alternating light–dark cycle until E21. Water and food were provided ad libitum throughout the experiment.

Tissue extraction

On E21, the pregnant rats were sedated and killed via cesarean section under anesthesia with the intraperitoneal injection of pentobarbital. In each case, the fetus was opened using a midline incision, and the presence of a left-sided diaphragmatic hernia was confirmed. The lung tissue was removed, with the left lung used for the analysis. All lungs were transversely dissected in a similar manner with symmetrical slices, and the medial portion of the lungs was fixed in 10 % formalin solution for 24 h and embedded in paraffin for the morphological analysis.

Histology and morphometric analysis

Formalin-fixed, paraffin-embedded, 4-l m-thick lung sections were stained with hematoxylin–eosin (HE). At least six photographs of randomly selected microscopic fields were analyzed per animal. The pulmonary alveolar wall thickness was assessed by measuring the thicknesses of five of the thinnest alveolar wall sections per field in * 50 fields per group, using a previously described method [16–18]. The quantitative lung morphometry assessment was performed using the NIH ImageJ software program at 2009 magnification.

Immunohistochemistry and pulmonary artery morphometry

Immunohistochemistry was performed using formalin-fixed, paraffin-embedded lung tissues. The primary antibodies included a mouse anti-proliferating cell nuclear antigen antibody (PCNA, Dako, 1:100), rabbit polyclonal antibody against surfactant protein-C (SP-C) (Santa Cruz, 1:200), monoclonal antibody to a smooth muscle actin (aSMA) (Sigma, 1:5000), and rabbit polyclonal antibody to green fluorescent protein (GFP) (Abcam, 1:500).

The number of PCNA-positive cells was manually counted using a grid with the assistance of the ImageJ software program and expressed as the percentage of positive staining cell over the total cell number/field. Cells with strong brown nuclear staining were considered to be PCNA-positive. Brown cytoplasmic cell staining was considered to indicate SP-C-positive cells. The number of SP-C-positive cells over the total cell number/field was also manually counted. Both the analyses of PCNA and SP-C were limited to the air exchanging parenchyma only, excluding large airways and vessels.

The thicknesses of medial walls of arteries stained with a-SMA antibodies were calculated using a formula previously described in the literature [19]. Only fully muscularized vessels with the external diameter less than 100 l m were included in the analysis [20].

Statistical analysis

The data were analyzed statistically using the IBM SPSS Statistic 20 software package. A one-way ANOVA and the Mann–Whitney U test were used in accordance with the data distribution. The Shapiro–Wilk test was used to confirm the normality of the data. A p value of \ 0.05 was considered to be statistically significant.

Results

Morphology and cell characteristics

The population of cells derived from the adult lung eGFP transgenic rats was expanded in the culture dish; the cells exhibited a spindle shape and fibroblast-like morphology (Fig. 1a). In addition, the cells had the ability to adhere to the tissue culture dish, with proliferation and growth into small colonies. The number of colonies of various sizes increased, demonstrating proliferation and expansion throughout the whole plastic surface until confluence (Fig. 1b). Passage 3 of the MSC culture displayed a monomorphic appearance with spindle cells in the culture. The cultured cells differentiated into three lineages, including osteoblasts, adipocytes, and chondroblasts in the in vitro study (data not shown).

Alveolar parenchymal morphology

The lung morphology of the fetuses in the CDH group was significantly different to that observed in the normal lungs based on an analysis of the alveolar wall thickness and alveolar air space area. The alveolar walls in the CDH group were thicker than those noted in the control group (10.84 l m, range 9.85–12.08 vs. 7.81 l m, range 7.18–8.58 l m, respectively; p = 0.000) (Fig. 2a; Table 1). Meanwhile, the alveolar air space area per field in the CDH group was smaller than that observed in the control group (0.028 mm^2, range 0.026–0.032 vs. 0.056 mm^2, range 0.053–0.061 mm^2, respectively; p = 0.000) (Fig. 2a; Table 1). MSC transplantation significantly decreased the alveolar wall thickness (8.77 l m, range 7.91–9.61 vs. 10.84 l m, range 9.85–12.08 l m,

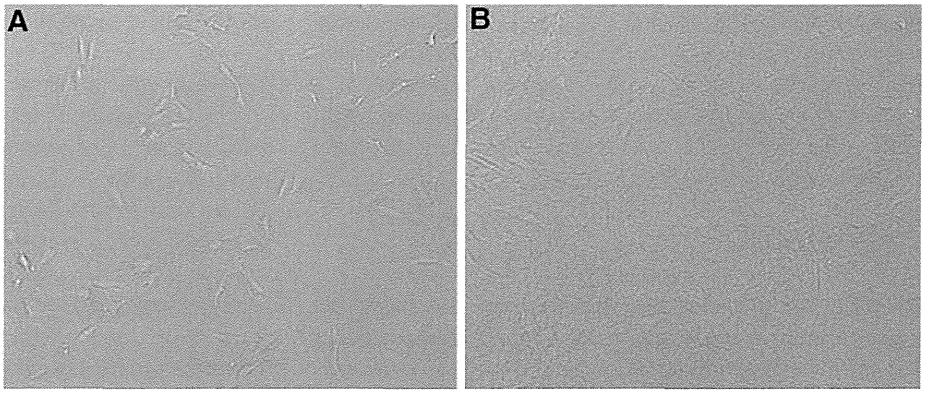

Fig. 1 Morphology of the mesenchymal stem cells in culture. a Appearance of the mesenchymal stem cell culture of passage 3 on day 3. b Passage 3 of the MSC culture on day 7 (magnification: a, b 9 100)

respectively; p = 0.000) and the increased alveolar air space area compared to that observed in the CDH group (0.041 mm^2, range 0.038–0.046 mm^2/field vs. 0.028 mm^2, range 0.026–0.032 mm^2/field, respectively; p = 0.000). The alveolar wall thicknesses in the MSC-treated CDH and control groups were 8.77 l m (range 7.91–9.61 l m) and 7.81 l m (range 7.18–8.58 l m; p = 0.000), respectively, while the alveolar air space area was 0.041 mm^2 (range 0.038–0.046 mm^2)/field and 0.056 mm^2 (0.053–0.061 mm^2/field; p = 0.000), respectively. These findings were consistent with the microscopic appearance, in which the lungs in the control group displayed well-developed saccules, thin alveolar walls and well-expanded air space areas. In contrast, the CDH lungs exhibited thickened alveolar walls with compacted tissue and undeveloped saccules.

Cell proliferation

Anti-proliferating cell nuclear antigen was used as a marker of cell proliferation. In the analysis, the immunoreactivity of PCNA was confined to the nucleus, with positive nuclei expressing strong brown staining. PCNA-positive cells were more numerous in the lung parenchyma of the control group than in that observed in the CDH group (Fig. 2b). In all groups, within the air exchanging parenchyma, PCNA-positive cells were mostly found in the interstitial areas of the lungs. The proportion of proliferating cells/field in the CDH group was significantly decreased compared to that observed in the control group, at 2.18 % ± 1.224 vs. 10.22 % ± 4.460/field, respectively (p = 0.000) (Fig. 3a). In addition, the proportion of PCNA-positive cells was significantly increased in the MSC-treated CDH group, at 8.32 % ± 4.018/field compared with the 2.18 % ± 1.224/field observed in the CDH group (p = 0.000). The proportion of PCNA-positive cells had no significant differences between the MSC-treated CDH group and the control group [8.32 % ± 4.018 vs. 10.22 % ± 4.460/field, respectively (p = 0.140)].

Lung maturation

Surfactant protein-C is a specific marker for alveolar type II cells. SP-C-positive cells were clearly visualized as brown cytoplasmically stained cells in the epithelial lining of the alveolar wall. In the CDH group, the SP-C expression was very faint and almost not detected (Fig. 2c). In addition, the proportion of SP-C-positive cells per field was significantly decreased in the CDH group compared with that observed in the control group, at 0.57 % ± 0.791 vs. 11.47 % ± 2.762/field, respectively (p = 0.000) (Fig. 3b). In contrast, MSC transplantation significantly enhanced the SP-C expression in the nitrofen-induced left-CDH fetuses, with the number of SP-C-positive cells being higher (10.16 % ± 2.912/field; p = 0.000) than that observed in the CDH group. In contrast, there were no significant differences in the SP-C expression between the control and MSC-treated CDH groups.

Pulmonary artery morphometry

The muscular layer of the arteries in the CDH group was thicker than that observed in the control group (Fig. 2d). In addition, the medial thickness index of the pulmonary arteries was significantly higher in the CDH group (0.25 ± 0.096) than in the control group (0.22 ± 0.070; p = 0.011) (Fig. 3c), while the medial thickness index of the arteries in the MSC-treated CDH group was significantly lower than that observed in the CDH group (0.22 ± 0.08 vs. 0.25 ± 0.096, respectively; p = 0.024). There were no significant differences in the medial thickness index between the control and the MSC-treated CDH groups (p = 0.933). The degree of medial hypertrophy relative to the external diameter is represented by the medial thickness index.

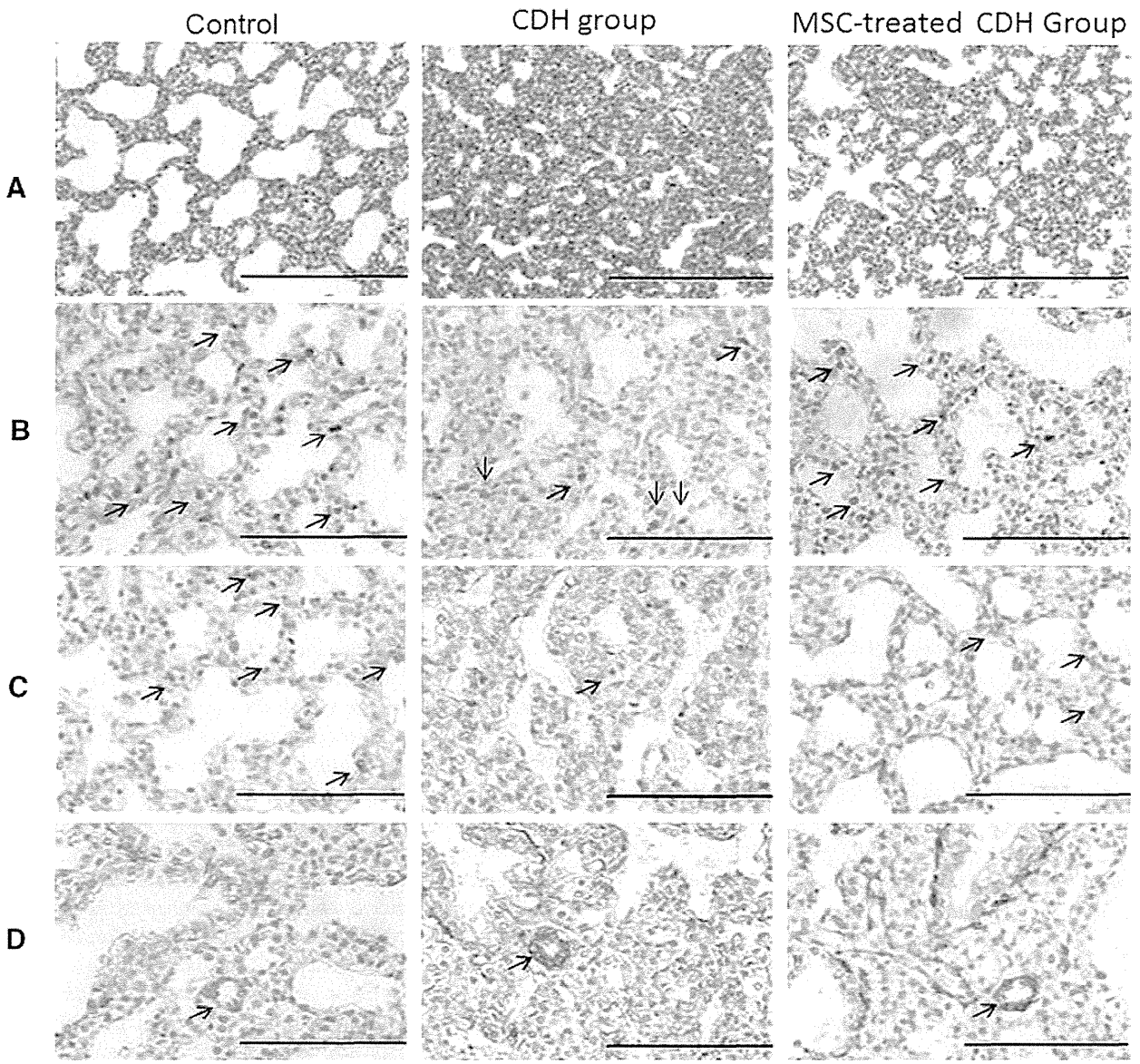

Fig. 2 Morphological analysis of HE staining and immunohistochemistry. Tissues stained with a Hematoxylin–eosin (HE). b Immunohistochemical staining for PCNA. The arrow indicates PCNA-positive cells. c Immunohistochemical staining for SP-C. The arrow indicates SP-C-positive cells. d Immunohistochemical staining for alpha smooth muscle actin. The arrow indicates the medial thickness in the pulmonary arteries (magnification: a 9 200, b–d 9 400). Scale bars a 200 l m, b–d 100 l m

Table 1 Morphometrical analysis of the lungs

Morphometrical analysis	Control	CDH	MSC-treated CDH
Alveolar wall thickness (l m)	7.81 l m (7.18–8.58)	10.84 l m (9.85–12.08)*	8.77 l m (7.91–9.61)*, #
Alveolar air space area (mm^2/field)	0.056 mm^2 (0.053–0.061)	0.028 mm^2 (0.026–0.032)*	0.041 mm^2 (0.038–0.046)*, #

The data are presented as the median (25th–75th percentile), * p\ 0.001, compared to the control group, # p\ 0.001, compared to the CDH group

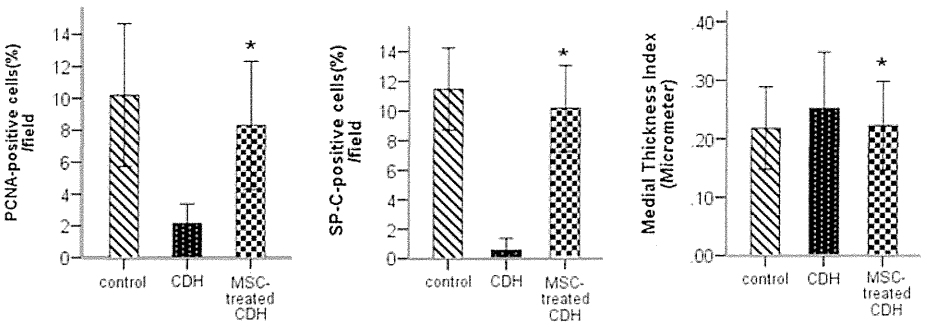

Fig. 3 Quantitative analysis of individual markers. The quantitative expression of proliferating cell nuclear antigen (a), surfactant protein-C (b), and the medial thickness index (a-SMA) (c) among the three groups. The data are presented as mean ± SD. *p\ 0.05 compared with the CDH group

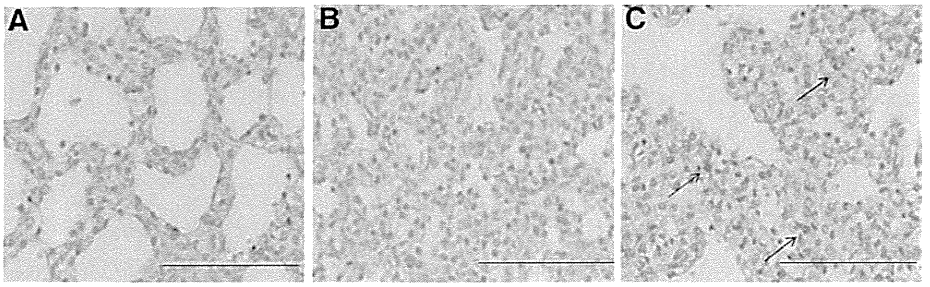

Fig. 4 Engraftment of the MSCs in the lung tissue. a Control group, b CDH group, c MSC-treated CDH group. In the MSC-treated CDH group, there was a positive GFP cell expression in the interstitial lungs (magnification a–c 9 400). Scale bars a–c 100 l m

Therefore, MSC therapy significantly decreased the degree of muscularization of the pulmonary arteries.

Mesenchymal stem cell engraftment

In the MSC-treated CDH group, the expression of green fluorescent protein (GFP)-positive cells was observed in the lung parenchyma (Fig. 4c), particularly in the interstitial areas of the lungs, presenting as brown-stained cells.

Discussion

Severely hypoplastic lung diseases and associated persistent pulmonary hypertension remain as serious causes of morbidity and mortality in CDH patients, despite advances in postnatal interventions, such as the advent of inhaled nitric oxide (iNO), extracorporeal membrane oxygenation (ECMO), high-frequency oscillatory ventilation (HFO) and gentle ventilation [1, 2]. The TOTAL trial requires additional time to investigate the efficacy of these treatments in terms of improving the morbidity of moderate and mortality of severe CDH [7, 8]. At present, half of fetuses cannot be salvaged with FETO [7]. One reason for this high mortality rate is that FETO simply does not trigger adequate lung development. Several reports have attempted to demonstrate the efficacy of peptides, hormones, and alternatives in experimental models of CDH, although the results have shown limited effects with respect to lung morphogenesis [3–6].

Recent advances in stem cell biology appear to be very promising and attractive, as such cells are unspecialized and/or undifferentiated, with the capacity for self-renewal and the power to give rise to multiple different specialized cell types [7, 21]. The activation of endogenous lung stem cells may increase the number and size of bronchopulmonary segments, whereas exogenous stem cells contribute to lung development [10]. Such cells may have a direct effect due to the integration, differentiation, and/or activation of resident stem cells via paracrine mechanisms [10]. The paracrine immunomodulation of stem cells and their protective effects against parenchymatous and vascular lung injury have previously been demonstrated in several models of lung injury [12, 19]. In particular, MSCs are ideal because they can modulate damage due to their potent immunosuppressive effects [10, 12, 22]. In addition, several experimental studies have shown that treatment with MSCs can reverse lung parenchymal fibrosis, pulmonary injury, and pulmonary hypertension [10, 12, 14]. However, it is important to note that MSCs represent a 'heterogeneous' population, expressing different levels of a panel of characteristic cell surface markers. MSCs are further defined by their properties of cell attachment, self-renewal, clonogenicity and the ability to differentiate towards multiple lineages [23, 24]. In the present study, cultured cells derived from the minced lungs of eGFP rats were found to have the capacity to adhere to the plastic culture surface, with a spindle-shape morphology, and both proliferative and clonogenic abilities. The cells also demonstrated the capability to

differentiate into osteoblasts, adipocytes, and chondroblasts in vitro; these characteristics reflect mesenchymal stem cell properties.

Cell-based therapy approaches to treating lung diseases have focused on using non-resident stem cells, particularly bone marrow MSCs (BMSCs); however, given the engraftment capacity of BMSCs after transplantation and the possible lung phenotypes after transplantation, there are inconsistent results as to whether BMSCs truly engraft and differentiate into lung phenotypes [14, 25]. Recent studies have also demonstrated the presence of "mesenchymal-like" progenitor cells in the lungs with a multipotent regenerative and high proliferative capacity, with the expectation that lung-derived MSCs will more easily respond to the local lung milieu, thus promoting engraftment and regeneration [12, 25]. Although it remains controversial, MSCs derived from various organs may exhibit tissue-specific differences with various epigenetic features.

Mesenchymal stem cells have the ability to transfer and engraft from maternal to the fetal body. Chen et al. [26] showed that human MSCs from maternal origin have the ability to traffic through the placenta to the fetal tissue in the pregnant rat model. Placenta expresses vascular endothelial growth factor A (VEGF-A) and it may be secreted into the fetal blood. The level of VEGF-A is higher in the fetal circulation than the maternal circulation, showing a concentration gradient from maternal to fetal circulation. High concentration of VEGF-A in the fetal blood may play a role in the mobilization of maternal circulating stem cells.

Nitrofen-induced CDH model rats demonstrate diaphragmatic defects, hypoplastic lungs and pulmonary vascular anomalies, in which the diaphragmatic defect is produced during the course of lung development [3–6]. Lung morphogenesis specifically requires an interaction between the epithelia and mesenchyme, identified as the epithelial–mesenchymal interaction [27]. The extent of induction is dependent on the amount of mesenchyme, and the proximal lung bud epithelium requires continuous stimulation from the distal mesenchyme. In the present study, the fetal lung hypoplasia appeared to have improved, as indicated by the enlargement of air space area and a decrease in the alveolar wall thickness. MSC transplantation may, therefore, enhance cell proliferation, as indicated by increases in the number of PCNA-positive cells and the SP-C expression. MSC transplantation may also decrease the degree of muscularization of the pulmonary arteries, as evidenced by the decrease in the medial thickness index. In addition, the expression of GFP-positive cells was observed in the mesenchyme of the lungs, and the proportion of GFP-positive cells/field seems lower than that of PCNA-positive cells/field in the MSC-treated CDH group. Based on these results, we hypothesize that the MSCs transplanted via the uterus vein engrafted into the fetal lung parenchyma, where they promoted the epithelial–mesenchymal interaction, thus ameliorating lung hypoplasia. However, there are several limitations associated with this study, as we did not perform a molecular biological study so as to identify the signaling pathways and/or elucidate the molecular roles of these cells in proliferation and differentiation. We are preparing to perform such studies in the near future.

Mesenchymal stem cells display a broad spectrum of potential effects, including immunomodulatory, antifibrotic, and trophic actions, on resident tissue progenitor cells, features that suggest the critical role of these cells in tissue homeostasis, and serve as the basis for their application in cellular therapy [12, 21, 24]. The therapeutic effects of MSCs in lung disease not only include their derived capacity to migrate to the sites of injured tissue, but also their ability to interact with injured host cells and secrete paracrine soluble factors that can alter the response of the endothelium and epithelium to injury via the release of growth factors [12–14, 28]. Indeed, the paracrine immunomodulation of MSCs and their protective effect against parenchymatous and vascular lung injury have previously been reported in several models of lung injury [10, 14, 15]. The main paracrine factors secreted by MSCs are growth factors and their corresponding receptors, some of which include VEGF, FGF, TGF, HGF, angiopoietin, etc. In addition these cells have the capacity to secrete cytokines and chemotactic factors, as well as regulatory peptides and stem cell-specific active factors; these soluble paracrine factors have various effects on the respiratory epithelium, endothelial cells, smooth muscle cells and fibroblasts in the lungs [29, 30]. Although, some studies have demonstrated the efficacy of treatment with amniotic-derived MSCs in nitrofen-induced CDH animal models, the mechanisms underlying both the development of lung damage and repair in the setting of CDH remain to be fully elucidated [31, 32].

Conclusion

The present results demonstrate that MSCs derived from adult rat lungs have the capacity of engraftment into the fetal lung parenchyma. Therefore, MSC transplantation may promote cell proliferation and differentiation in nitrofen-induced CDH model rats, thus suggesting that MSC therapy may have therapeutic potential to ameliorate pulmonary hypoplasia and pulmonary hypertension.

Acknowledgments The authors wish to thank Mr. Brian Quinn for supporting the manuscript. This work was supported in part by a Grant-in-Aid for Scientific Research from the Japanese Society for the Promotion of Science.

Conflict of interest The authors do not have any conflicts of interest related to this paper.

References

1. Masumoto K, Teshiba R, Esumi G, Nagata K, Takahata Y, Hikino S, Hara T, Hojo S, Tsukimori K, Wake N, Kinukawa N, Taguchi T (2009) Improvement in the outcome of patients with antenatally diagnosed congenital diaphragmatic hernia using gentle ventilation and circulatory stabilization. Pediatr Surg Int 25:487–492
2. Nagata K, Usui N, Kanamori Y, Takahashi S, Hayakawa M, Okuyama H, Inamura N, Fujino Y, Taguchi T (2013) The current profile and outcome of congenital diaphragmatic hernia: a nationwide survey in Japan. J Pediatr Surg 48:738–744
3. Takayasu H, Nakazawa N, Montedonico S, Sugimoto K, Sato H, Puri P (2007) Impaired alveolar epithelial cell differentiation in the hypoplastic lung in nitrofen-induced congenital diaphragmatic hernia. Pediatr Surg Int 23:405–410
4. Esumi G, Masumoto K, Teshiba R, Nagata K, Kinoshita Y, Yamaza H, Nonaka K, Taguchi T (2011) Effect of insulin-like growth factors on lung development in a nitrofen-induced CDH rat model. Pediatr Surg Int 27:187–192
5. Gonzalez-Reyes S, Alvarez L, Diez-Pardo JA, Tovar JA (2003) Prenatal vitamin E improves lung and heart hypoplasia in experimental diaphragmatic hernia. Pediatr Surg Int 19:331–334
6. Schmidt AF, Gonçalves FLL, Regis AC, Gallindo RM, Lourenço S (2012) Prenatal retinoic acid improves lung vascularization and VEGF expression in CDH rat. Am J Obstet Gynecol 207:76.e25–76.e32
7. Deprest J, De Coppi P (2012) Antenatal management of isolated congenital diaphragmatic hernia today and tomorrow: ongoing collaborative research and development. J Pediatr Surg 47:282–290
8. Jani J, Nicolaides KH, Keller RL, Benachi A, Peralta CF, Favre R, Moreno O, Tibboel D, Lipitz S, Eggink A, Vaast P, Allegaert K, Harrison M, Deprest J, Antenatal-CDH-Registry Group (2007) Observed to expected lung area to head circumference ratio in the prediction of survival in fetuses with isolated diaphragmatic hernia. Ultrasound Obstet Gynecol 30:67–71
9. Jani J, Valencia C, Cannie M, Vuckovic A, Sellars M, Nicolaides KH (2011) Tracheal diameter at birth in severe congenital diaphragmatic hernia treated by feto endoscopic tracheal occlusion. Prenat Diagn 31:699–704
10. de Coppi Paolo, Deprest Jan (2012) Regenerative medicine for congenital diaphragmatic hernia: regeneration for repair. Eur J Pediatr Surg 22:393–398
11. Hematti P (2008) Role of mesenchymal stromal cells in solid organ transplantation. Transpl Rev 22:262–273
12. Hoffman AM, Paxson JA, Mazan MR, Davis AM, Tyagi S, Murthy S, Ingenito EP (2011) Lung-derived mesenchymal stromal cell post-transplantation survival, persistence, paracrine expression, and repair of elastase-injured lung. Stem Cells Dev 20:1779–1792
13. Zhu X, Shi W, Tai W, Liu F (2012) The comparison of biological characteristics and multilineage differentiation of bone marrow and adipose derived mesenchymal stem cells. Cell Tissue Res 11:277–287
14. Aslam M, Baveja R, Liang OD, Fernandez-Gonzalez A, Lee C, Mitsialis SA, Kourembanas S (2009) Bone marrow stromal cells attenuate lung injury in a murine model of neonatal chronic lung disease. Am J Respir Crit Med 180:1122–1130
15. van Haaften T, Thébaud B (2006) Adult bone marrow derived stem cell for the lung: implications for pediatric lung disease. Pediatr Res 59:94–99
16. Pua JZ, Stonestreet BS, Cullen A, Shahsafaei A, Sadowska GB, Sunday ME (2005) Histochemical analyses of altered fetal lung development following single vs multiple courses of antenatal steroids. J Histochem Cytochem 53:1469–1479
17. Wu S, Platteau A, Chen S, McNamara G, Whitsett J, Bancalari E (2010) Conditional overexpression of connective tissue growth factor disrupts postnatal lung development. Am J Respir Cell Mol Biol 42:552–563
18. Kitaguchi Y, Taraseviciene-Stewart L, Hanaoka M, Natarajan R, Kraskauskas D, Voelkel N (2012) Acrolein induces endoplasmic reticulum stress and causes airspace enlargement. PLoS One 7(5):e38038. doi:10.1371/journal.pone.0038038
19. Hansmann G, Fernandez-Gonzalez A, Aslam M, Vitali SH, Martin T, Mitsialis SA, Kourembanas S (2012) Mesenchymal stem cell-mediated reversal of bronchopulmonary dysplasia and associated pulmonary hypertension. Pulm Circ 2:170–181
20. Okoye BO, Losty PD, Lloyd DA, Gosney JR (1998) Effect of prenatal glucocorticoids on pulmonary vascular muscularisation in nitrofen-induced congenital diaphragmatic hernia. J Pediatr Surg 33:76–80
21. Pozzobon M, Ghionzoli M, De Coppi P (2010) ES, iPS, MSC, and AFS cells. Stem cells exploitation for pediatric surgery: current research and perspective. Pediatr Surg Int 26:3–10
22. Crisostomo PRM, Markel TA, Wang Y, Meldrum DR (2008) Surgically relevant aspects of stem cell paracrine effects. Surgery 143:577–581
23. Ardhanareeswaran K, Miratsou M (2013) Lung stem and progenitor cells. Respiration 85:89–95
24. Keating A (2012) Mesenchymal stromal cells: new directions. Stem Cell 10:709–716
25. Ingenito EP, Tsai L, Murthy S, Tyagi S, Mazan M, Hoffman A (2012) Autologous lung-derived mesenchymal stem cell transplantation in experimental emphysema. Cell Transpl 21:175–189
26. Chen CP, Lee MY, Huang JP, Aplin JD, Wu YH, Hu CS, Chen PC, Li H, Hwang SM, Liu SH, Yang YH (2008) Trafficking of multipotent mesenchymal stromal cells from maternal circulation through the placenta involves vascular endothelial growth factor receptor-1 and integrins. Stem Cells 26:550–561
27. Badri L, Walker NM, Ohtsuka T, Wang Z, Delmar M, Flint A, Golden MP, Toews GB, Pinsky DJ, Krebsbach PH, Lama VN (2011) Epithelial interactions and local engraftment of lung-resident mesenchymal stem cells. Am J Respir Cell Mol Biol 45:809–816
28. Lee JW, Fang X, Krasnodembskaya A, Howard JP, Matthay MA (2011) Concise review: mesenchymal stem cells for acute lung injury: role of paracrine soluble factors. Stem Cells 29:913–919
29. Zhu F, Xia ZF (2013) Paracrine activity of stem cells in therapy for acute lung injury and adult respiratory distress syndrome. J Trauma Acute Care Surg 74:1351–1356
30. Conese M, Carbone A, Castellani S, Gioia SD (2013) Paracrine effects and heterogeneity of marrow-derived stem/progenitor cells: relevance for the treatment of respiratory diseases. Cell Tissues Organs 197:445–473
31. Di Bernardo J, Maiden MM, Hershenson MB, Kunisaki SM (2014) Amniotic fluid derived mesenchymal stem cells augment fetal lung growth in a nitrofen explant model. J Pediatr Surg. doi:10.1016/j.jpedsurg.2014.01.013
32. Pederiva F, Ghionzoli M, Pierro A, De Coppi P, Tovar JA (2013) Amniotic fluids stem cells rescue both in vitro and in vivo growth, innervation, and motility in nitrofen-exposed hypoplastic rat lungs through paracrine effects. Cell Transpl 22:1683–1694

PLOS | ONE

RESEARCH ARTICLE

Derivation of Mesenchymal Stromal Cells from Pluripotent Stem Cells through a Neural Crest Lineage using Small Molecule Compounds with Defined Media

Makoto Fukuta[1,2,3.], Yoshinori Nakai[4.], Kosuke Kirino[5.], Masato Nakagawa[6], Kazuya Sekiguchi[1,2,7], Sanae Nagata[2], Yoshihisa Matsumoto[1,2,3], Takuya Yamamoto[6,8], Katsutsugu Umeda[9], Toshio Heike[9], Naoki Okumura[10], Noriko Koizumi[10], Takahiko Sato[4], Tatsutoshi Nakahata[5], Megumu Saito[5], Takanobu Otsuka[3], Shigeru Kinoshita[4], Morio Ueno[4]*, Makoto Ikeya[2]*, Junya Toguchida[1,2,7]*

1. Department of Tissue Regeneration, Institute for Frontier Medical Sciences, Kyoto University, Kyoto, Japan, 2. Department of Cell Growth and Differentiation, Center for iPS Cell Research and Application, Kyoto University, Kyoto, Japan, 3. Department of Orthopaedic Surgery, Graduate School of Medical Sciences, Nagoya City University, Nagoya, Japan, 4. Department of Ophthalmology, Kyoto Prefectural University of Medicine, Kyoto, Japan, 5. Department of Clinical Application, Center for iPS Cell Research and Application, Kyoto University, Kyoto, Japan, 6. Department of Reprogramming Science, Center for iPS Cell Research and Application, Kyoto University, Kyoto, Japan, 7. Department of Orthopaedic Surgery, Graduate School of Medicine, Kyoto University, Kyoto, Japan, 8. Institute for Integrated Cell-Material Sciences (WPI-iCeMS), Kyoto University, Kyoto, Japan, 9. Department of Pediatrics, Graduate School of Medicine, Kyoto University, Kyoto, Japan, 10. Department of Biomedical Engineering, Faculty of Life and Medical Sciences, Doshisha University, Kyotanabe, Japan

*mueno@koto.kpu-m.ac.jp (MU); mikeya@cira.kyoto-u.ac.jp (MI); togjun@frontier.kyoto-u.ac.jp (JT)

. These authors contributed equally to this work.

OPEN ACCESS

Citation: Fukuta M, Nakai Y, Kirino K, Nakagawa M, Sekiguchi K, et al. (2014) Derivation of Mesenchymal Stromal Cells from Pluripotent Stem Cells through a Neural Crest Lineage using Small Molecule Compounds with Defined Media. PLoS ONE 9(12): e112291. doi:10.1371/journal.pone.0112291

Editor: Maurilio Sampaolesi, Stem Cell Research Institute, Belgium

Received: March 24, 2014

Accepted: October 6, 2014

Published: December 2, 2014

Funding: This work was supported in part by Grants-in-Aid for Scientific Research from JSPS (#25293320), a grant from Core Center for iPS Cell Research, Research Center Network for Realization of Regenerative Medicine from JST, and the Leading Project for Realization of Regenerative Medicine from MEXT to MI and JT. MI was also supported by the Adaptable and Seamless Technology Transfer Program through target-driven R&D, Exploratory Research from JST (AS242Z00931P). JT was also supported by the Center for Clinical Application Research on Specific Disease/Organ from JST. MU was also supported by Grants-in-Aid for Scientific Research from JSPS (#20791288). The funders had no role in the study design, data collection and analysis, decision to publish, or preparation of the manuscript.

Competing Interests: The authors have declared that no competing interests exist.

Abstract

Neural crest cells (NCCs) are an embryonic migratory cell population with the ability to differentiate into a wide variety of cell types that contribute to the craniofacial skeleton, cornea, peripheral nervous system, and skin pigmentation. This ability suggests the promising role of NCCs as a source for cell-based therapy. Although several methods have been used to induce human NCCs (hNCCs) from human pluripotent stem cells (hPSCs), such as embryonic stem cells (ESCs) and induced pluripotent stem cells (iPSCs), further modifications are required to improve the robustness, efficacy, and simplicity of these methods. Chemically defined medium (CDM) was used as the basal medium in the induction and maintenance steps. By optimizing the culture conditions, the combination of the GSK3b inhibitor and TGFb inhibitor with a minimum growth factor (insulin) very efficiently induced hNCCs (70–80%) from hPSCs. The induced hNCCs expressed cranial NCC-related genes and stably proliferated in CDM supplemented with EGF and FGF2 up to at least 10

passages without changes being observed in the major gene expression profiles. Differentiation properties were confirmed for peripheral neurons, glia, melanocytes, and corneal endothelial cells. In addition, cells with differentiation characteristics similar to multipotent mesenchymal stromal cells (MSCs) were induced from hNCCs using CDM specific for human MSCs. Our simple and robust induction protocol using small molecule compounds with defined media enabled the generation of hNCCs as an intermediate material producing terminally differentiated cells for cell-based innovative medicine.

Introduction

In order to apply human pluripotent stem cells (hPSCs) to innovative medicine, such as cell therapy, disease modeling, and drug discovery, robust and efficient methods to produce the desired cell types without contaminating undesired cells are indispensable [1]. Since the contamination of hPSCs, in particular, may cause serious adverse effects, careful monitoring, which requires a considerable amount of time and cost, has to be conducted. Therefore, it would be beneficial to have intermediate cells between hPSCs and terminally differentiated cells, which are proved to have no contaminated hPSCs, contain limited but multiple differentiation properties, and stably proliferate without phenotypic changes. One of the promising candidates with such features is the neural crest cell (NCC) [2].

The neural crest emerges at the border of the neural and non-neural ectoderm in gastrula embryos during vertebrate development [3]. Cells in the neural crest, and later in the dorsal part of the neural tube, eventually delaminate and migrate throughout the body while retaining their characteristic phenotype [4]. When they reach their target tissues, NCCs differentiate into specific cell types depending on the location [5]. NCCs give rise to the majority of cranial bone, cartilage, smooth muscle, and pigmented cells in the cranial region, as well as neurons and glia in the peripheral nervous system [3–5]. Cardiac NCCs are known to contribute to valves in the heart, while vagal NCCs differentiate into enteric ganglia in the gut [6]. NCCs give rise to neurons and glia in the peripheral nervous system in the trunk region, secretory cells in the endocrine system, and pigmented cells in the skin.

Using a lineage-tracing system, rodent neural crest-derived cells were detected in adult tissues such as bone marrow, and still retained multipotent differentiation properties, which indicated that these cells are one of the cell-of-origin of multipotent mesenchymal stromal cells (MSCs) [7, 8]. Therefore, the production of human MSCs (hMSCs) from hPSCs via NCC lineage is a promising approach for the use of hPSCs in innovative medicine [9, 10]. A considerable number of studies have been dedicated to establishing robust and efficient induction methods from hPSCs to hNCCs in the past decade [11–13]. However, most of these studies used non-human stromal feeder cells or only achieved low induction

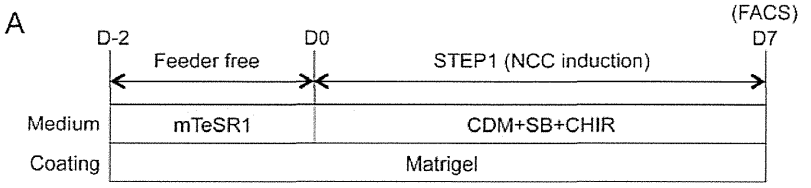

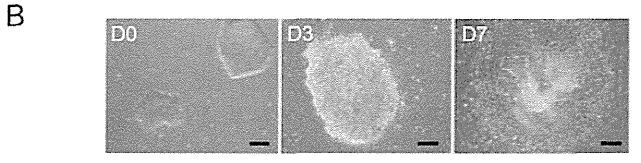

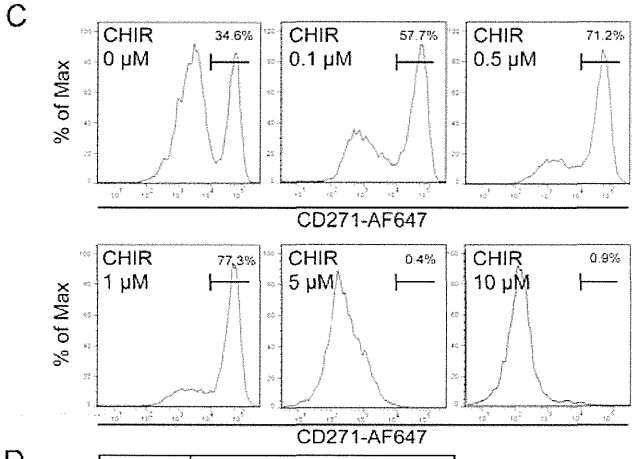

D

Cell	Induction efficiency (%)
414C2	73.5 ± 6.0
201B7	79.8 ± 2.6
KhES1	75.7 ± 4.4
KhES3	71.4 ± 4.8
H9	75.0 ± 6.2

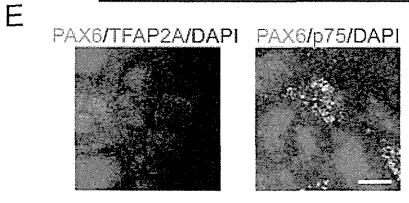

Figure 1. Induction of $p75^{high}$ cells from hPSCs. A) Schematic representation of the protocol. B) Morphology of colonies during the induction. Phase contrast images were taken on days 0, 3, and 7. Scale bar, 200 nm. C) The fraction of p75-positive cells in 201B7 cells was treated with SB431542 (SB) (10 nM) and CHIR99021 (CHIR) (indicated concentration) for seven days, stained with an anti-p75 antibody, and analyzed by FACS. D) Fraction of the $p75^{high}$ population induced by SB (10 nM) and CHIR (1 nM) from hESCs (KhES1, KhES3, H9) and hiPSCs (414C2, 201B7). Average ± SD. N= 3, biological triplicate. E) Immunocytochemical analyses of colonies on day 7 (201B7). Cells were stained with antibodies against PAX6, TFAP2A, and p75. Scale bar, 100 nm.

doi:10.1371/journal.pone.0112291.g001

efficiencies. An ideal method from the standpoint of clinical applications is free from xeno-materials, such as feeder cells or serum, and can be performed using a chemically defined medium (CDM). Two groups have published protocols that are compatible with these requirements [14, 15]. The first group employed a two-step approach, in which hPSCs were firstly dissociated into single cells and cultured with CDM for two weeks for the adaptation. Cells were then cultured with CDM that was supplemented with an activator of Wnt signaling and inhibitor of Activin/Nodal/TGFb signaling, but was free from BMP signaling modulation [14]. The other group used MEF-conditioned hESC media for the initial step, and replaced it with knockout serum replacement (KSR)-based medium, which thereafter was gradually replaced with an increasing amount of N2 media. They employed an inhibitor for BMP signaling in addition to an inhibitor for Activin/Nodal/TGFb signaling during the initial 3 days, and then replaced them with an activator of Wnt signaling [15]. Therefore, the requirement for signal modulators, particularly BMP signaling inhibitors, remains controversial. Further modifications are still needed to improve the robustness, efficacy, and simplicity of these methods.

We here developed a robust and efficient induction protocol using CDM containing inhibitors for TGFb signaling and GSK3b, but not for BMP signaling with minimal growth factors. The protocol very efficiently induced hNCCs (70–80%) from hPSCs irrespective of the type (hESCs vs hiPSCs) or generating method (viral-integrated vs plasmid-episomal). Genome-wide analyses revealed that induced hNCCs retained their gene expression profile as NCCs even after 10 passages. As for differentiation properties, induced hNCCs successfully differentiated into peripheral neurons, glia, melanocytes and corneal endothelial cells. In addition, induced hNCCs were able to produce cells comparable to hMSCs, which were free from contaminated hPSCs and could differentiate into osteo-, chondro-, and adipogenic cells. Furthermore, using iPSCs generated and maintained under feeder-free and xeno-free culture systems, we successfully induced hNCCs, hMSCs, and osteogenic cells using chemically defined media.

Materials and Methods

Ethics statement

The experimental protocols dealing human subjects were approved by the Ethics Committee of the Department of Medicine and Graduate School of Medicine, Kyoto University. Written informed consent was provided by each donor.

Cell lines

hESCs (H9, KhES1, and KhES3) and hiPSCs (414C2 and 201B7) were used in this study [16–19] They were maintained on SNL feeder cells [20] in Primate ES cell medium (ReproCELL, Tokyo, Japan) supplemented with 4 ng/ml recombinant human FGF2 (WAKO, Osaka, Japan). 987A3, hiPSCs generated and maintained

under feeder-free and xeno-free culture systems from human primary fibroblasts, were maintained on iMatrix-551 (rLN511E) (Nippi, Tokyo, Japan)-coated cell culture plates with StemFit (Ajinomoto, Tokyo, Japan) as described previously [21]. Bone marrow derived hMSCs were obtained from donors and used in our previous study [22]. Human corneal endothelial cells were isolated from human corneal tissues obtained for research purpose from SightLife (Seattle, WA, USA).

Culture media and reagents

mTeSR1 medium (STEMCELL Technology, Vancouver, Canada) was used for the feeder-free culture of PSCs. The induction and maintenance of hNCCs were performed using previously reported CDM [23], which contains Iscove's modified Dulbecco's medium/Ham's F-12 1:1, 1x chemically defined lipid concentrate (GIBCO, Grand Island, NY, USA), 15 mg/ml apo-transferrin (Sigma, St. Louis, MO, USA), 450 mM monothioglycerol (Sigma), 5 mg/ml purified BSA (99% purified by crystallization; Sigma), 7 mg/ml Insulin (WAKO), and penicillin/streptomycin (Invitrogen, Carlsbad, CA, USA). Culture dishes were coated with growth factor-reduced Matrigel (BD, Bedford, MA, USA) or fibronectin (Millipore, Bedford, CA, USA). EGF (R&D, Minneapolis, USA) and FGF2 were used to maintain hNCCs [24]. SB431542 (SB) (Sigma), CHIR99021 (CHIR) (WAKO), BMP4 (R&D), DMH1 (Tocris, Bristol, UK), LDN193189 (Stemgent, Cambridge, MA, USA), and recombinant human Noggin (R&D) were used to modulate growth factor signals. Retinoic acid (RA) (Sigma) was used to modulate hNCCs.

Fluorescence-Activated Cell Sorting (FACS)

FACS was performed by AriaII (BD) according to the manufacturer's protocol. The antibodies used in FACS were listed in Table S1. In all experiments, FACS histograms of isotype controls were similar to those without antibodies; therefore, histograms without antibodies were used as control populations.

Immunocyto- and immunohistochemistry

Prior to performing immunostaining with antibodies, cells on plates were fixed with 4% paraformaldehyde at 4℃ for 15 minutes, washed two times with PBS, and incubated with 0.3% TritonX100 at 4℃ for 30 minutes as the surface-active agent for penetration processing, and any nonspecific binding was blocked with 2% skim milk/PBS at 4℃ for 1 hour. Cornea samples obtained from rabbits euthanized three days after the injection of cells were fixed with 4% paraformaldehyde and incubated in 1% bovine serum albumin (BSA) (Sigma) to block other bindings. DAPI (1:5000; Sigma) was used to counterstain nuclei. The primary antibodies used in this study were summarized in Table S1. The observation and assessment of samples were performed with BZ-9000E (Keyence, Osaka, Japan).

RT-PCR and qPCR

Total RNA was purified with the RNeasy Mini kit (Qiagen, Valencia, CA, USA) and treated with the DNase-one kit (Qiagen) to remove genomic DNA. One microgram of total RNA was reverse transcribed for single-stranded cDNA using a random primer and Superscript III reverse transcriptase (Invitrogen), according to the manufacturer's instructions. PCR was performed with ExTaq (Takara, Shiga, Japan). Quantitative PCR with the Thunderbird SYBR qPCR Mix (TOYOBO, Osaka, Japan) was performed using the StepOne real-time PCR system (Applied Biosystems, Forester City, CA, USA) in duplicate or triplicate. Primer sequences were listed in Table S2.

cDNA microarray

Total RNA was prepared using the RNeasy Mini Kit (Qiagen). cDNA was synthesized using the GeneChip WT (Whole Transcript) Sense Target Labeling and Control Reagents kit as described by the manufacturer (Affymetrix, Santa Clara, CA, USA). Hybridization to the GeneChip Human Gene 1.0 ST expression arrays, washing, and scanning were performed according to the manufacturer's protocol (Affymetrix). Expression values were calculated using the RMA summarization method and the data obtained were analyzed by GeneSpring GX 11.5.6 (Agilent Technologies, Santa Clara, CA, USA) for correlation coefficients, scatter plots, a volcano plot, heat maps, and hierarchical clustering (Distance metrics: Pearson's Centered, Linkage rule: Average). Differentially expressed genes were identified by statistical analyses and fold changes. Statistical analyses were performed using a one-way ANOVA with a Benjamini and Hochberg False Discovery Rate (BH-FDR 5 0.01) multiple testing correction followed by Tukey HSD post hoc tests (GeneSpring GX). Microarray data have been submitted to the Gene Expression Omnibus (GEO) public database at NCBI, and the accession number is GSE 60313. Data for hBM90, 91, and 94 have already been described [22]. Data from GSE44727 and GSE45223 were used for a comparison analysis in Figure S3.

Differentiation of hPSC-derived hNCCs

Peripheral neuronal differentiation

Sorted hNCCs were cultured in CDM supplemented with 10 mM SB and 1 mM CHIR as a sphere using the hanging drop technique (16 10^4 cells per sphere) as previously described [25]. Twenty-four hours after the hanging drop culture, spheres were plated onto Polyornithine/laminin/fibronectin (PO/Lam/FN)-coated plates in DMEM/F12 (Invitrogen) supplemented with 1 x N2 supplement (GIBCO), 1 x GlutaMAX (Invitrogen), 20 ng/ml FGF2, and 20 ng/ml EGF. These cells were cultured for two days under these conditions and the medium was then replaced with DMEM/F12 supplemented with 1 x N2 supplement, 1 x GlutaMAX, and 10 ng/ml BDNF (R&D), GDNF (R&D), NT-3 (R&D), and NGF (R&D). The medium was changed every 3 days and passages were performed every week [26].

Differentiation was confirmed by immunostaining for peripherin, Tuj-1, and GFAP 3 weeks after induction.

Melanocyte differentiation

Cells were plated onto fibronectin-coated dishes in CDM supplemented with 10 mM SB and 1 mM CHIR. Melanocyte induction was performed the next day with CDM supplemented with 1 mM CHIR, 25 ng/ml BMP4, and 100 nM endothelin-3 (American Peptide Company, Sunnyvale, CA, USA) [15, 27, 28]. The medium was changed every other day. Differentiation was confirmed by induction of the MITF and c-KIT genes on day 7.

Corneal endothelial cell differentiation

Cells were induced to corneal endothelial cells with corneal endothelial cell-conditioned CDM. Conditioned CDM was derived by collecting medium from cultured human corneal endothelial cells [29]. The selective ROCK inhibitor Y-27632 (WAKO) was used on the first day of the induction. The medium was changed every two days, and cells were analyzed by immunocytochemistry after twelve days. RT-qPCR was performed 3, 5, and 8 days after the induction.

Induction of hMSCs from hNCCs

Cells were plated onto tissue culture dishes (BD) at a density of 6.56 10^4 cell/cm^2 in CDM supplemented with 10 mM SB and 1 mM CHIR. The medium was replaced the next day with aMEM (Nacalai Tesque, Tokyo, Japan) supplemented with 10% fetal bovine serum (FBS) (Nichirei Inc., Tokyo, Japan) [14, 26]. The morphology of cells started to change approximately 4 days after the induction. Passages were performed every week using 0.25% trypsin-EDTA (GIBCO) at a density of 16 10^4 cells/cm^2. hMSC markers (CD73, CD44, CD45 and CD105) were analyzed by FACS 14 days after the hMSC induction. We used STK2 (DS Pharma Biomedical, Osaka, Japan) as the MSC medium and tissue culture dishes coated with fibronectin for the hMSC induction under chemically defined media conditions.

Differentiation of hNCC-derived hMSCs

Osteogenic differentiation

A total of 2.56 10^5 induced hMSCs/well were seeded on 6-well dishes (BD) and cultured in osteogenic induction medium, aMEM, 10% FBS, 0.1 mM dexamethasone, 50 ng/ml ascorbic acid, and 10 mM b-glycerophosphate for 2 weeks for osteogenic differentiation [24]. STK3 (DS Pharma) was used as the osteogenic induction medium instead of the osteogenic induction medium to achieve osteogenic differentiation under chemically defined media conditions. The culture medium was changed every other day for 1 week. Differentiation properties were confirmed by the formation of calcified nodules, as detected with Alizarin Red staining. Briefly, culture wells were washed twice in phosphate-buffered saline (PBS) and fixed for 10 minutes at room temperature in 100% ethyl alcohol. The

Alizarin Red solution (40 mM, pH 4.2) was applied to the fixed wells for 10 min at room temperature. Non-specific staining was removed by several washes with water.

Chondrogenic differentiation

Two-dimensional chondrogenic induction was performed as previously described [30]. Briefly, cells (1.56 10^5) that induced hMSCs were suspended in 5 ml of chondrogenic medium (DMEM: F12 (Invitrogen), 1% (v/v) ITS1 mix (BD), 0.17 mM AA2P, 0.35 mM Proline (Sigma), 0.1 mM dexamethasone (Sigma), 0.15% (v/v) glucose (Sigma), 1 mM Na-pyruvate (Invitrogen), 2 mM GlutaMax, and 0.05 mM MTG supplemented with 40 ng/ml PDGF-BB and 1% (v/v) FBS (Nichirei)), and were subsequently transferred to fibronectin-coated 24-well plates (BD). A total of 1 ml of the chondrogenic medium was added after 1 hour. TGFb3 (R&D) was subsequently added at 10 ng/ml on days 3 to 6, and BMP4 was added to a concentration of 50 ng/ml on day 10. Micromass cultures were maintained at 37°C under 5% CO_2 and 5% O_2 for 16 days. Differentiation properties were confirmed by Alcian Blue staining. Briefly, induced cells were fixed for 30 minutes with 10% formalin (Sigma) and rinsed with PBS. These cells were then stained overnight with Alcian Blue solution (1% Alcian Blue (MUTO PURE CHEMICAL CO., LTD, Tokyo, Japan) in 3% glacial acetic and 1% HCl, pH 1) and destained with the acetic acid solution.

Adipogenic differentiation

Cells were seeded onto 6-well tissue culture dishes at a density of 5.06 10^5 cells/well for adipogenic differentiation, and were cultured in aMEM containing 10% FBS, 1 mM dexamethasone, 10 mg/ml insulin, and 0.5 mM isobutylxanthine for 3 weeks [31]. Induced cells were fixed in 10% formalin for 1 hour at room temperature, followed by 20 minutes in 0.3% Oil Red O staining solution (Sigma).

Results

Derivation of $p75^{high}$ cells from hPSCs

To transfer hPSCs from feeder to feeder-free culture conditions, colonies were dissociated into small cell clumps (about 10 cells/clumps) by pipetting several times, seeded on matrigel-coated dishes (2–4 clumps/cm^2), and cultured with mTeSR1 medium for two days. hNCC induction was then initiated by substituting CDM supplemented with chemicals (Figure 1A). Cells gradually migrated from colonies and proliferated during the induction (Figure 1B). Cells were harvested after 7 days of being induced, and were subsequently sorted according to the expression of p75 (Figure 1C). We detected two peaks in p75-positive populations, designated $p75^{low}$ and $p75^{high}$, and the efficiency of hNCC induction was evaluated based on the fraction of $p75^{high}$ cells.

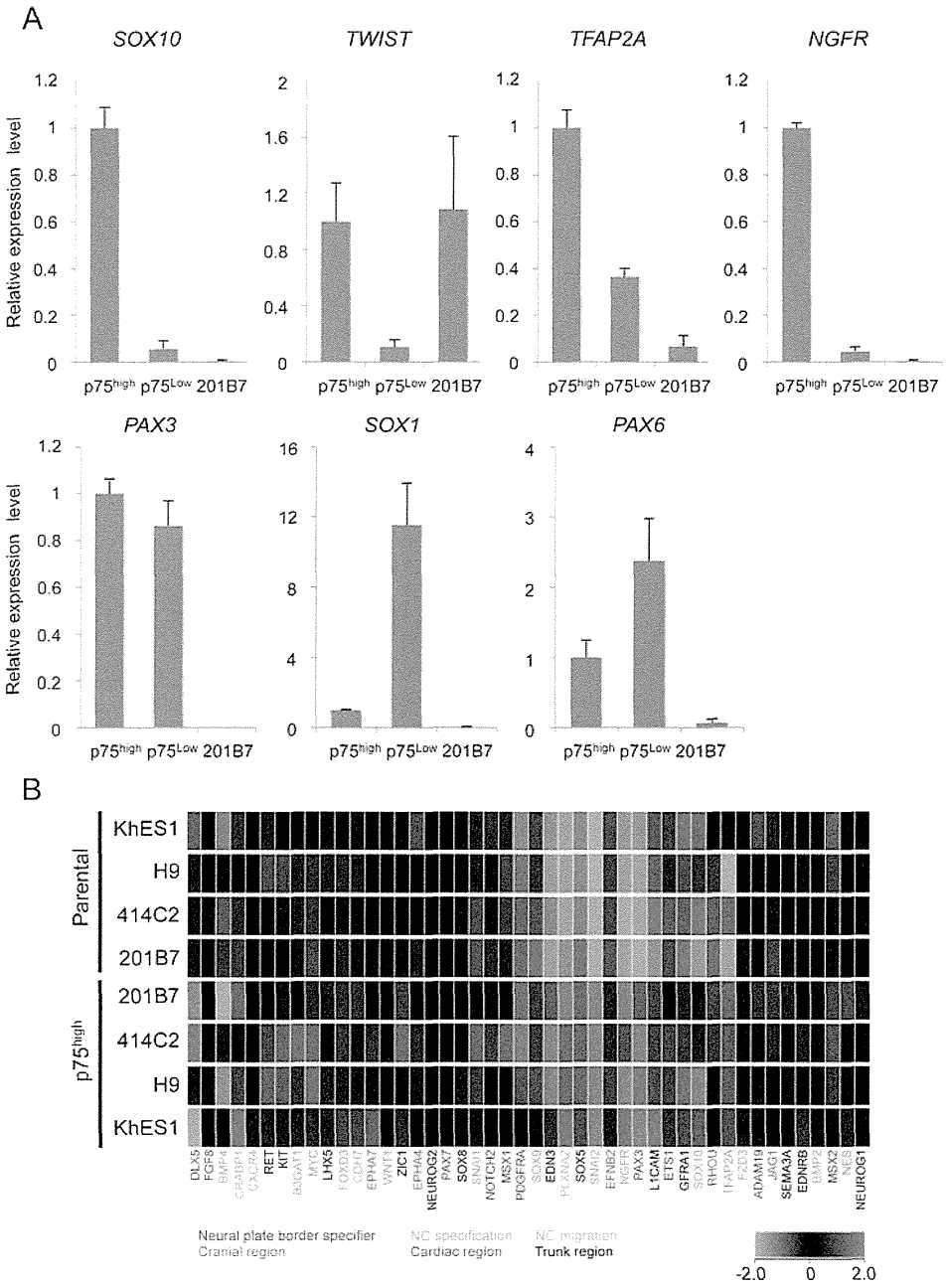

Figure 2. Expression profiles of sorted p75^{high} cells. A) The expression of marker genes in sorted p75^{high} and p75^{low} cells. The mRNA expression of each gene was analyzed by RT-qPCR in undifferentiated 201B7 (hiPSCs) and sorted p75^{low} and p75^{high} cells, and was shown as a relative value using the level in sorted p75^{high} cells as 1.0. Average ± SD. N5 3, biological triplicates. B) Clustering analyses of NCC markers in p75^{high} populations from several hESC and hiPSC lines. Marker genes for each sub-population of NCCs were labeled using the indicated colors.

doi:10.1371/journal.pone.0112291.g002

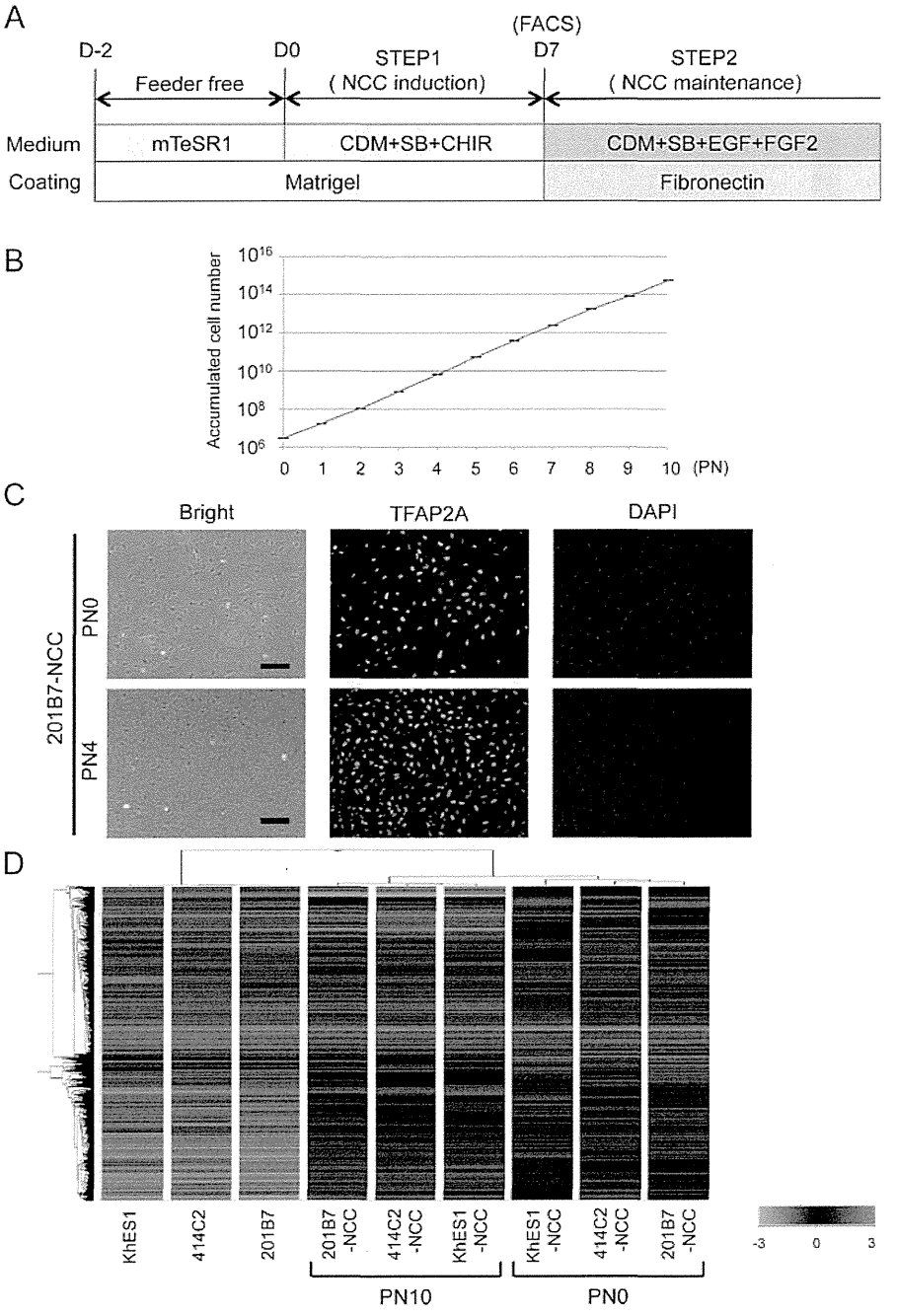

Figure 3. Sustained expansion of hNCCs with original characteristics. A) Schematic representation of the culture conditions. B) Growth profile of 201B7-derived hNCCs. Average ± SD. N5 3, biological triplicate. C) Phase contrast images and immunostaining of TFAP2A in 201B7-derived hNCCs at PN0 and PN4, Scale bar, 200 nm. D) Hierarchical clustering analyses of hPSCs and hPSC-derived hNCCs at PN0 and PN10.

doi:10.1371/journal.pone.0112291.g003